Precipitation changes during the Maya collapse reflected in cuticle morphology

Jesse James Hennekam

December 2013

MSc Research
Earth, Life and Climate

Supervisors:
Prof. Wagner-Cremer F.
Dr. Hoek W.Z

Department of Earth Sciences and Physical Geography
Section Palaeoecology
Laboratory of Palaeobotany and Palynology
Institute of Earth Sciences,
Utrecht University, The Netherlands

Universiteit Utrecht

Abstract

Cuticle analysis is used as a paleo-precipitation proxy in boreal and subtropical environments. Here, this method has been applied successfully in the tropical Maya Lowlands (Tabasco, Mexico). Multiple proxies have already indicated the presence of severe drought episodes during the time of the Maya Collapse. By applying cuticle analysis on fossil leaf material originating from the Maya Lowlands, a new independent proxy is used for investigating these drought episodes. Epidermal cell density of fossil leaf remains from the family *Fabaceae* are used to achieve a reconstruction of past precipitation changes between 620 and 1013 AD. The result of this research corresponds well with speleothem records from Yok Ballum Cave (Belize) and the sediment record of Lake Chichancanab (Yucatan Peninsula, Mexico). By analysing the results, we conclude that climatic change in form of a decrease in precipitation was occurring during and after the demise of the Maya Civilisation.

Introduction

For thousands of years the Maya culture flourished in the southern part of Mexico, until it suddenly disappeared between 750 and 900 AD (Lowe, 1985). Although this so called Terminal Classic Period (TCP) has been intensively investigated, the cause of this event remains a highly debated topic and is not fully understood. It is speculated that climatic changes during that time period may have been linked with this Maya collapse (Gunn, 1981; Dahlin, 1983; Folan, 1985; Curtis, 1996). Research in lake sediments from Mexico provided the first evidence of a period of multiple drought events during the TCP (Hodell, 1995; Hodell, 2005), which eventually could have contributed to the disappearance of the Maya culture in Central America. Several other studies using lake sediments and speleothem records as a proxy support the hypothesis of relatively dry conditions and or a series of drought events during the TCP (Haug, 2003; Metcalfe, 2010; Stahle, 2011; Lachniet, 2012; Kennett, 2012). These studies, however, do not seem to agree on the exact timing of this drought event. Also, the fluctuations within the severity of the drought period shown by these proxies seem to vary, as well as the duration of the event. $\delta^{18}O$ and sulphur concentrations measured in Lake Chinchananab (Yucatan Peninsula, Mexico) indicate that the drought episode ended around 925 AD, whereas speleothem records from Yok Balum Cave (Belize) suggest that conditions remained dry until 1200 AD. Another difference between these two proxies is the fluctuations seen in the record. Whereas the lake sediments indicate a relatively stable drought period, the speleothem record shows a more fluctuating pattern, interpreted by the author as proof for multiple drought episodes during a period of time.

Northern Hemisphere climate in the Americas are mainly characterized by wet and dry seasons. The occurrence of wet seasons is mostly during the summer months, whereas dry seasons are typical for the winter. Some places, however, have a reversed climate, showing more precipitation during the winter combined with low precipitation in the summer months (Baya California Peninsula). In the southern part of Mexico (Isthmus of Tehuantepec and eastward on) precipitation seems to occur throughout the year. The Mid-Summer Drought (MSD) is a phenomenon in the annual precipitation cycle of Southern Mexico. During the MSD, a relative minimum in precipitation is reached during the wet summer months. This

change is expected to be related with changes in Sea Surface Temperature (SST) in the Pacific. Precipitation during the Madden-Julian oscillation (Molinari *et al*., 1997) is enhanced in the Caribbean, resulting in strengthening of the trade winds and the formation of tropical storms in the Eastern Pacific and relative drought (MSD) in Southern Mexico.

Prolonged periods of drought have been observed in northern Mexico in the twentieth century. These drought episodes during the summer coincided with wet conditions in the southern part of Mexico. These events occur due to the negative phase of the Pacific decadal oscillation (PDO) (Méndez and Magaña, 2010). However, the positive phase of the PDO results in strengthening of the Caribbean low-level jet and therefore decreases the precipitation in South Mexico.

El Niño/Southern Oscillation (ENSO) has a large impact on climate fluctuations in Mexico. Due to the position of Mexico, the effects of ENSO differ within the country. Whereas, during the dry season (November till April), El Niño years are characterized by a significant increase of precipitation in the north-western part of Mexico, a reversed pattern is observed at the Isthmus of Tehuantepec. Precipitation in this part of Mexico decreases drastically during El Niño winter months. With the Inter Tropical Convergence Zone (ITCZ) shifting southward, trade winds become more intense. This strengthening of the trade winds influences the formation of tropical cyclones in the Intra Americas Seas (IAS). The absence of tropical storms in combination with the reduction in humidity often results in extreme drought events in Mexico. Such an event occurred in 1997-1998 (Magaña et al., 2003), which resulted in forest fires and significant losses in agriculture and fisheries. During La Niña summers an ITCZ forms in Southern Mexico, resulting in the enhancement of precipitation of this area and causes drought in northwestern Mexico.

The Isthmus of Tehuantepec during the winter months is influenced by the passage of midlatitude frontal systems propagating in the IAS. These systems result in the formation of tropical storm in the Caribbean and create Northerns (Trasviña and Barton, 1997); high winds coming from the northwest. The amount of Northerns has a negative correlation with the precipitation in the Isthmus of Tehuantepec. One of the explanations of this phenomenon is that due to the lack of time, not enough moisture can be taken up into the atmosphere to produce precipitation when the next system crosses.

Most of the water available in the Maya Lowlands is derived from precipitation in the mountainous area in the south, the Chiapas Highlands. Two rivers, the Grijalva River and the Usumacinta River, transport the water from the highlands towards the Maya Lowlands. As both El Niño winter months as the appearance of Northerns result in the decrease of precipitation in the south of Mexico, the drought event taking place around 800 AD could have been influenced by one or both of these factors.

Drought stress signals in leafs have recently been linked to pinpoint drought events in time by combining cuticle analysis and carbon dating. By sampling modern and fossil leaf material in the Maya Lowlands, this material can then be used to test plant sensitivity to precipitation changes (modern) and the applicability of fossil leaf remains as a proxy for past drought episodes around 800 AD. This method
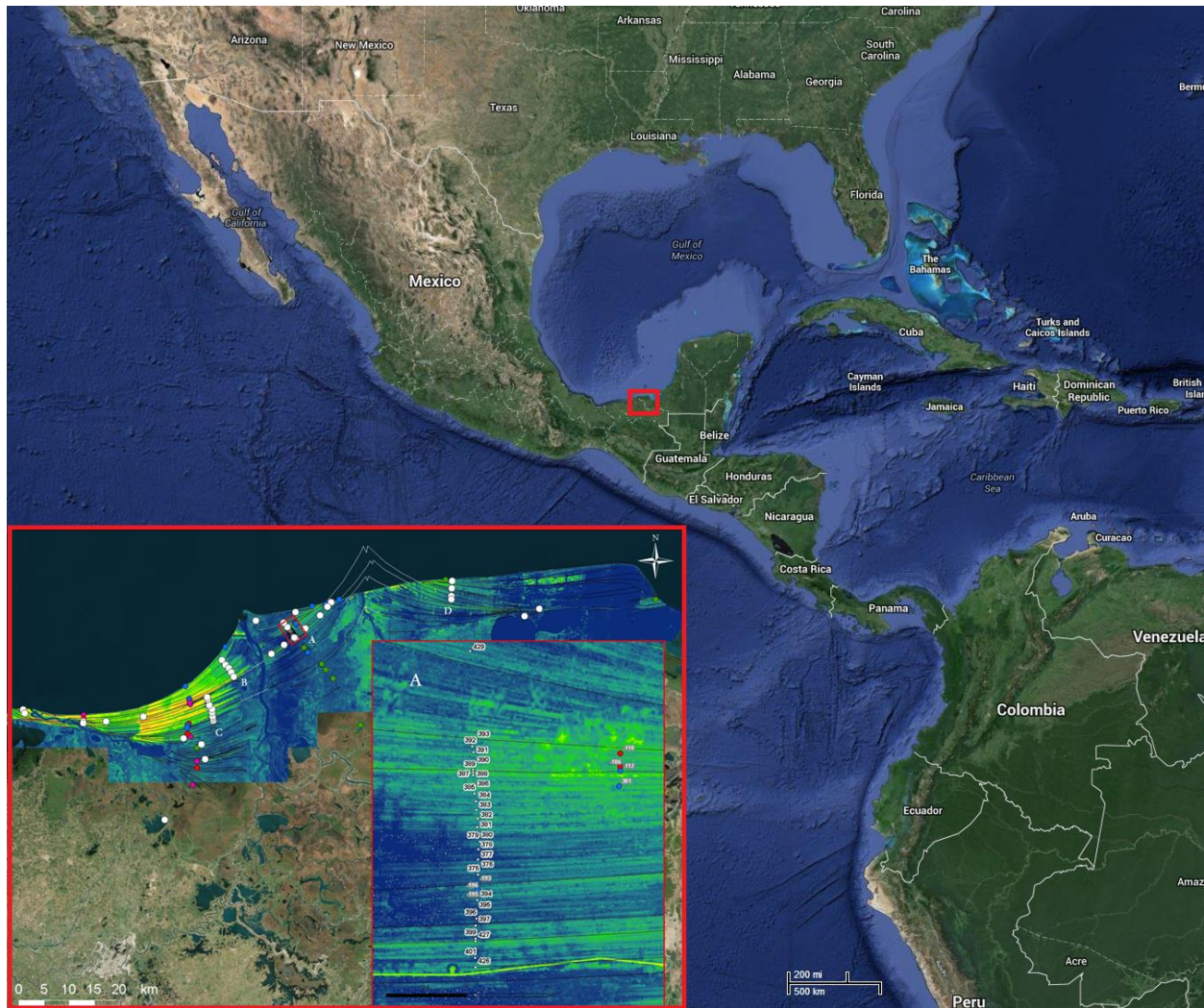
Figure 1 : Location of the Maya Lowlands, Left lower corner shows zoomed LIDAR image of the Maya Lowlands. Fieldwork transect A has been enlarged in the LIDAR image and is plotted on the right of the image.

has been developed by LPP-staff from the Utrecht University, Prof. Rike Wagner-Cremer, and has been successfully applied on leaf material from Florida already (Wagner et al., 2010). The analysis can be used for reconstructing humidity changes and changes in atmospheric CO_2 concentrations in the area during the past 5000 years. Such a reconstruction will result in a greater understanding of the climatic conditions prevalent when the Maya culture thrived.

The Maya Lowlands are ideal for this type of research as sites available for multi-proxy analysis of climate change are plentiful. Multiple cores have been taken in the area of Tabasco, Mexico. This area is considered to contain the largest beach ridge plain in the world, including ridges of over 5000 years old. The development of these ridges is dependent on abundant sediment supply and a repetitive formational agent (Psuty, 1965). Continuous coastal progradation combined with the sediment supply of the Usumacinta and the Grijalva river systems created this series of subparallel ridges and swales in the Maya Lowlands. Previous fieldwork has shown that these formations and the interlaying swales can

contain organic leaf material. Material from these ridges is used in this research for cuticle analysis based reconstruction of precipitation changes in the past.

Material and Methods

Site description

Transects, covering a large area of the Maya Lowlands, were cored over a period of three weeks. A total of 73 cores were collected, including 44 cores containing organic material. Besides 16 individual cores, four transects have been cored (Transects A, B, C and D). The location of these transects has been determined by using LIDAR images of the area combined with known OSL and radiocarbon datings, as certain time periods may be of interest based on historical events.

In this research, the focus lies on transect A (figure 1 and 3); a three kilometer long area located east of the Grijalva River, close to the town Frontera. A total of 38 cores were taken at Transect A, with 100 meter intervals between the cores and a depth ranging between the 3 and 11 meters. Of those 38 cores, 33 contained organic material. As organic leaf material is needed for reconstructing the past humidity values in this area, as well be required for ^{14}C dating, the cores lacking organic material created hiatuses in the transect. Therefore, three meter cores have been performed in the swales adjacent to all cores that lacked organic material, in order to decrease the gap in the record caused by these cores.

Age assessment

Assuming the sequence of beach ridges to be constant over time, ^{14}C dating has indicated that 100 meters contains roughly 25 years, showing that transect A covered a time period of around 750 years. With two ^{14}C datings in the middle of the transect showing a calendar age 773 and 783 AD, the transect is most likely to contain the time period between 500 and 1250 AD. When including an OSL date taken at transect A, this time period seems to be smaller than expected from the ^{14}C dating. A calendar age of 900 AD has been found, whereas, according to the ^{14}C dates, this age should have been around 1200 AD. The time period over which the beach ridges were formed assumed by the radiocarbon dates could therefore be incorrect. Possibly a variation in formation time occurs during this transect, unfortunately, more calendar ages have yet to be determined in order to support this hypothesis. Although both ^{14}C and OSL dating have an error propagation of around 100 years, both methods still suggest that the expected drought period should be included in the transect A.

In order to achieve a chronological reconstruction of humidity in this area, only material ranging within a depth between groundwater and three meters below surface has been investigated. When drilling in a beach ridge deep enough, multiple beach ridges can be included in one core. This is due to the formation of the ridges being similar to dune formation (figure 2). As sedimentation rate is unknown to be constant, shallow samples will be less affected by fluctuations due to sedimentation. Subsequently, the chances of unknowingly analysing the same beach ridge in multiple cores decreases. Whenever no

usable organic material was present at this depth range, only the shallowest organic layer has been investigated instead.

In transect A, four cores did not contain usable organic material within the three meter boundary, although in all these cores organic layers have been found within four meters below ground surface. This depth range has been set due to the high amount of organics in almost every core at this range, as well as the condition of the material, which seems to be less affected by degradation, compared to deeper units. Additionally, the effects of variations in sedimentation rate to the suggested calendar age of the material are less pronounced.
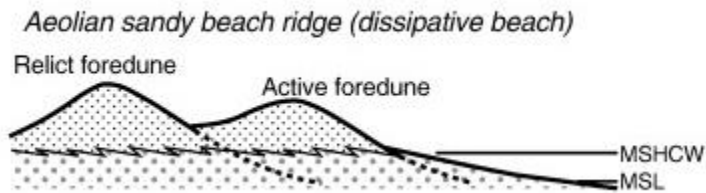

Fig. 2 : Schematic illustration showing the proposed formation of an aeolian sandy beach ridge. When coring in the ridges, samples from an older ridge can be obtained in the core due to the deposition of the younger ridge (Tamura T., 2012).

Using the OSL calendar age of one core and the radiocarbon derived ages from two other cores, an age model has been reconstructed by interpolating the three ages. In order to enhance this age model, more radiocarbon and OSL records are currently being investigated.

sample code	age estimate (AD)	Fabacea samples used	*Salix* samples used
393 290 300 320 I	1013,2475	1	
390 330 I	977,726	1	
389 330 I	962,403	1	
387 400 I	954,045	1	
386 240 I	940,115	1	
385 300 I	921,3095	1	
383 + 180 I	892,753	1	
381 225	863,5		2
380 - 155	850,2665	3	
380 - 170	848,8735	4	
379 275	838,426	1	1
378 170	824,496	1	1
376 290 I	791,7605	1	
193 171 L	766,6865	4	
196 315 L	754,4281	2	
397 160 + 180 I	693,554	1	
426 255 I	621,118		1

Table 1 : Sample codes of cores containing leaf material used in this research. Age estimate is in years AD and based on the interpolation of three dated points within the transect A.
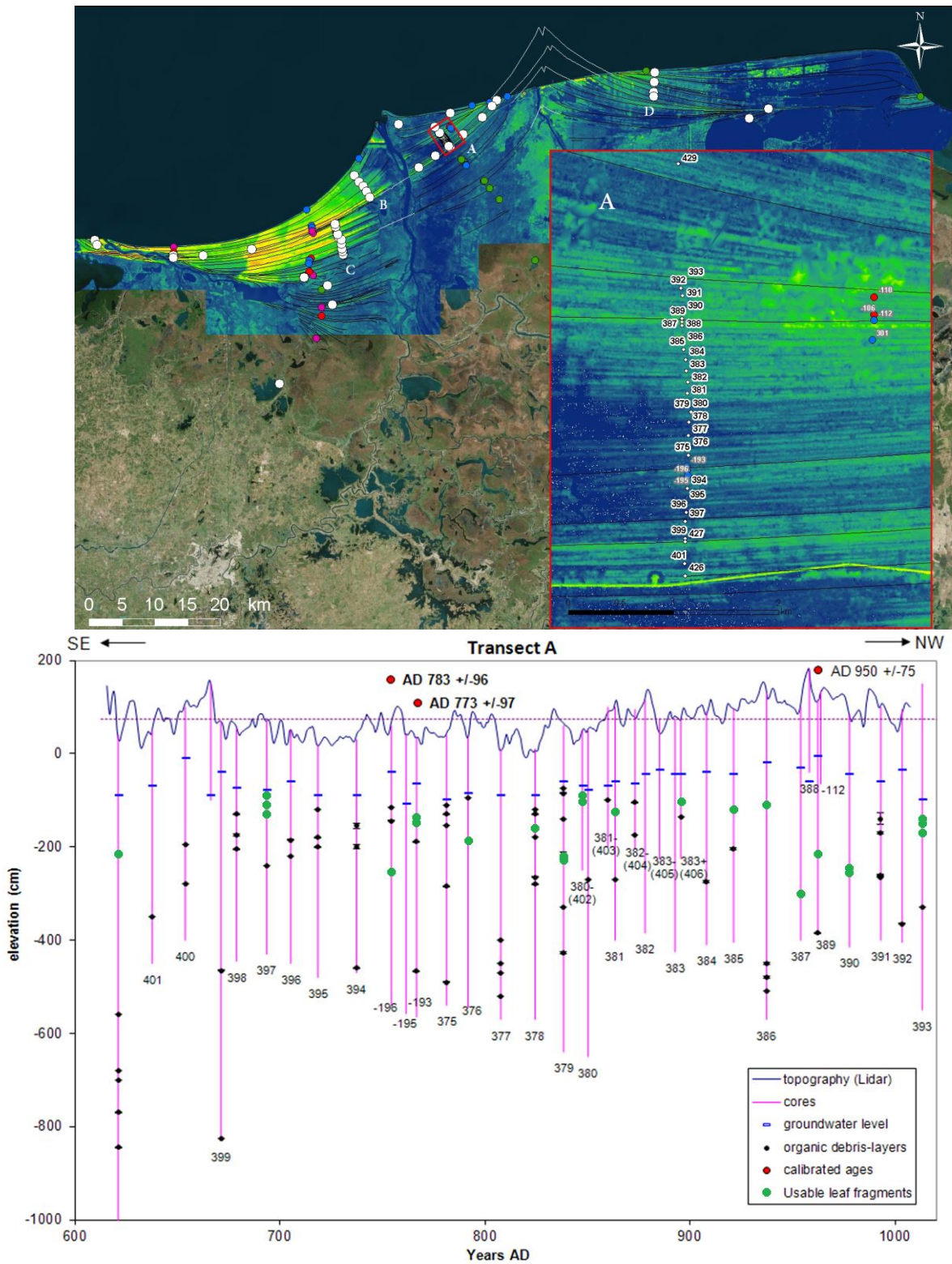
Fig. 3 : (Top) LIDAR Image of the fieldwork area at the Usumacinta and Grijalva floodplains, Tabasco, Mexico. Cores used in this research are shown in the bottom right of the image (transect A). (bottom) transect A, showing core depths, LIDAR elevation pattern, groundwater level, calibrated ages and the depth of leaf fragments used for cuticle analysis.

The leaf material present in the organic layers has been separated at Utrecht University, The Netherlands, by Kees Nooren. A concentration of 5% potassium hydroxide was added to the organic layers and heated at 70 °C for one hour. Subsequently, the material was sieved with a 335 µm sieve and washed using distilled H_2O. The leaf material was then separated by hand using a stereomicroscope.

First, the separated leaf material was crudely determined by using color characteristics and venation. In preparation for the microscopic analysis, an average of three pieces of leaf from every sample was bleached in 4% sodiumhypochlorite for a several minutes before being fixed upon a sample slide. The time of bleaching needed, strongly depended on the type of species and degradation rate of the material. Separation of the lower cuticle was not possible due to the fragility of the material. Therefore, the entire sample was stained with Saffranine. Glycerin jelly has been used to mount the cover glass on the stained sample slide.

An Olympus BH-2 research microscope (Utrecht, The Netherlands), combined with the program AnalySIS were used to measure various morphological aspects of the sampled leaf material. In general, a 1000x multiplier zoom was used; creating an area of field of 184,84 µm by 137,08 µm. Where possible, stomata density (SD) and epidermal cell density (ED) was determined at seven different leaf bearing alveoles on each leaf sample. With this data, the stomatal index (SI) can be calculated (Salisbury, 1927):

$$SI = \frac{SD}{SD + ED} * 100$$

Stomata length, stomata pore length and the guard cell width has been measured on 15 stomata, next to the area (CA) and circumference (CC) of 20 adjacent epidermal cells. The CA en CC were used in the following equation to derive undulation index (UI) (Kürschner, 1997):

$$UI = \frac{CC}{\sqrt{CA/\pi)}) * 2\pi}$$

Results

Samples

Multiple organic layers have been investigated, spread over a range of cores. Most of the investigated samples are dated after 800 AD and are estimated to have originated from a dry period. Samples before older than 800 AD are expected to point towards relatively more wet conditions.

Fabaceae code	Years (AD)	Mean SI	Stdev SI	Mean SD	Stdev SD	Mean ED	Stdev ED	Mean PL	Stdev PL	Mean SL	Stdev SL	Mean CA	Stdev CA	Mean CC	Stdev CC	Mean UI	Stdev UI
393 290 300 320 I	1013,2	11,13	1,69	500,00	38,46	4038,46	528,76	14,55	1,42	21,27	1,74	108,53	40,8	50,29	11,48	1,36	0,51
390 330 I	977,73	8,33		348,86		3837,43		15,66	1,46	24,05	1,26	195,2	41,28	67,95	9,48	1,37	0,42
389 330 I	962,4	9,28	0,53	294,87	22,21	2884,62	167,65	13,26	1,95	18,39	2,99	256,16	69,32	78,82	12,99	1,39	0,44
387 400 I	954,05	6,31	0,08	269,23	0,00	4000,00	54,39	13,88	1,74	27,25	2,36	154,86	35,05	58,61	7,1	1,33	0,34
386 240 I	940,12	10,98	2,12	368,13	76,46	2934,07	93,46	13,78	1,52	21,54	1,37	240,68	48,28	73,91	9,24	1,34	0,38
385 300 I	921,31	13,64	1,37	494,51	60,52	3126,37	88,03	15,46	2,15	24,37	2,5	201,76	52,71	66,23	9,64	1,32	0,37
383 + 180 I	892,75	11,08	0,60	307,69	0,00	2474,36	145,61	13,31	1,64	21,57	1,25	190,37	41,15	74,57	14,6	1,52	0,64
380 - 155 I, II, IV	850,27	8,83	1,06	265,38	59,14	4255,56	367,07	14,20	1,54	21,78	1,89	168,94	42,74	65,96	12,01	1,43	0,52
380 - 170 I, II, III, IV	848,87	11,98	0,99	365,82	39,35	2767,19	148,34	14,53	1,56	22,22	2,22	294,84	102,27	81,76	16,13	1,36	0,47
379 275 II	838,43	9,25	1,63	317,31	65,69	3096,15	49,65	13,68	1,53	23,64	2,83	267,47	70,68	86,82	16,22	1,50	0,54
378 170 II	824,5	8,43	0,67	338,46	42,13	3669,23	268,68	15,01	1,64	23,32	1,69	241,21	62,5	83,59	15,77	1,52	0,56
376 290 I	791,76	9,96	0,35	269,23	0,00	2435,90	96,79	15,1	2,13	22,84	1,59	296,95	77,09	86,57	16,38	1,42	0,53
193 171 1, 7A, 7B, 9	766,69	9,92	1,29	316,86	46,04	2904,90	166,94	10,41	1,07	15,34	1,47	251,66	83,36	73,81	13,42	1,34	0,42
196 315 2 A, 2B	754,43	13,56	1,83	173,08	27,83	1096,15	59,61	12,88	1,475	19,225	1,825	1003,22	358,86	152,56	31,47	1,36	0,47
397 160 + 180 I	693,55	10,34	1,29	115,38	0,00	1015,38	150,44	14,53	2,49	22,9	1,98	927,11	157,36	150,48	16,48	1,39	0,37

Salix code	Years (AD)	Mean SI	Stdev SI	Mean SD	Stdev SD	Mean ED	Stdev ED	Mean PL	Stdev PL	Mean SL	Stdev SL	Mean CA	Stdev CA	Mean CC	Stdev CC	Mean UI	Stdev UI
381 225 I, II	863,5	14,38	1,70	302,20	58,41	1788,46	116,88	13,17	1,95	27,53	2,47	609,06	102,95	134,17	15,09	1,54	0,42755
379 275 I	838,43	10,73	1,61	208,79	48,94	1719,78	173,03	15,32	1,82	24,98	1,26	600,17	154,61	142,92	27,95	1,65	0,6341
378 170 I	824,5	14,85	0,69	214,29	30,26	1142,86	139,94	10,69	1,38	28,83	1,46	969,11	242,07	179,38	23,58	1,63	0,42753
426 255 I	621,12	21,95	2,88	390,11	41,12	1395,60	138,17	11,79	1,33	24,99	2,37	463,72	109,73	126,43	22,87	1,66	0,61588

Tabel 2 : Measurement results; Upper table contains Fabaceae material, lower table contains *Salix* material. First number in sample code is GPS location point, second number in sample code is depth in mm, measured from surface. Age model is derived from two ¹⁴C datings and one OSL dating within the transect.

Determination of the material

Most of the leaf fragments used in this research appears to belong to the Family Fabaceae. Unfortunately, these samples could only be determined on family level. Being the third largest plant family in the world, the variety within Fabaceae seems enormous. Most of these plants present in the Maya Lowlands seem to be shrub or herb like. Hypothesizing the original flora to be similar to the present flora, we expect nowadays abundant plants to have also flourished in the past, and therefore possibly included in the core samples.

Due to the low variability in taxonomic features within Fabaceae, it is an unreliable characteristic for separating certain species (Idu et al., 1999). Fortunately, due to this same phenomenon, separation of the species seems unnecessary for applying cuticle analysis, providing no species specific adaptations for drought stress are present. Nevertheless, recent material investigated showed significant variability present in epidermal cell and stomatal cell density between species of Fabaceae present in the Maya Lowlands.

Characteristics in leaf morphology

Characteristics have been defined in order to determine whether or not a certain leaf fragment belongs to a certain group within the family Fabaceae or possibly other groups of plants. Pre-bleaching determination included variations in the venation of the material. Fabaceae material show a palmate venation; showing veins starting to spread towards the leaf edges at the location where the petiole is attached. A secondary characteristic derived was the colour of the material before the bleaching. Fabaceae material contained a rather unique brown/orange colour, which could easily be recognized without any optical instruments. Using the venation and colour characteristics, the leaf material could be roughly grouped before bleaching. The advantage of this method is that by doing so, not all the material needs to be bleached and, consequently, can still be used for carbon dating.
Once bleached and mounted, the material was then investigated under a microscope. Although in some cases difficult, the following characteristics have been used in order to identify the material: Stomata shape and size, epidermal cell shape, guard cell shape, placement of epidermal cells with respect to the stomata cell and guard cells, visibility of the stomata pore and the relative differences between the subsidiary cells on one side of the stomata compared to the cells on the other side.

Type 1, Fabaceae

Fabaceous species seem to be present in most of the organic layers and distinguishable from the other leaf material before bleaching the leaves. Type 1 was present in 14 organic layers and although the condition of the material varied, every layer had at least one measurable leaf fragment. When comparing with modern material investigated, type 1 closely resembles the *Inga vera*. Nevertheless, the SD and ED are considered higher in the *Inga vera*. Possibly, the determination is incorrect, or the variation could be explained by taphonomic processes.
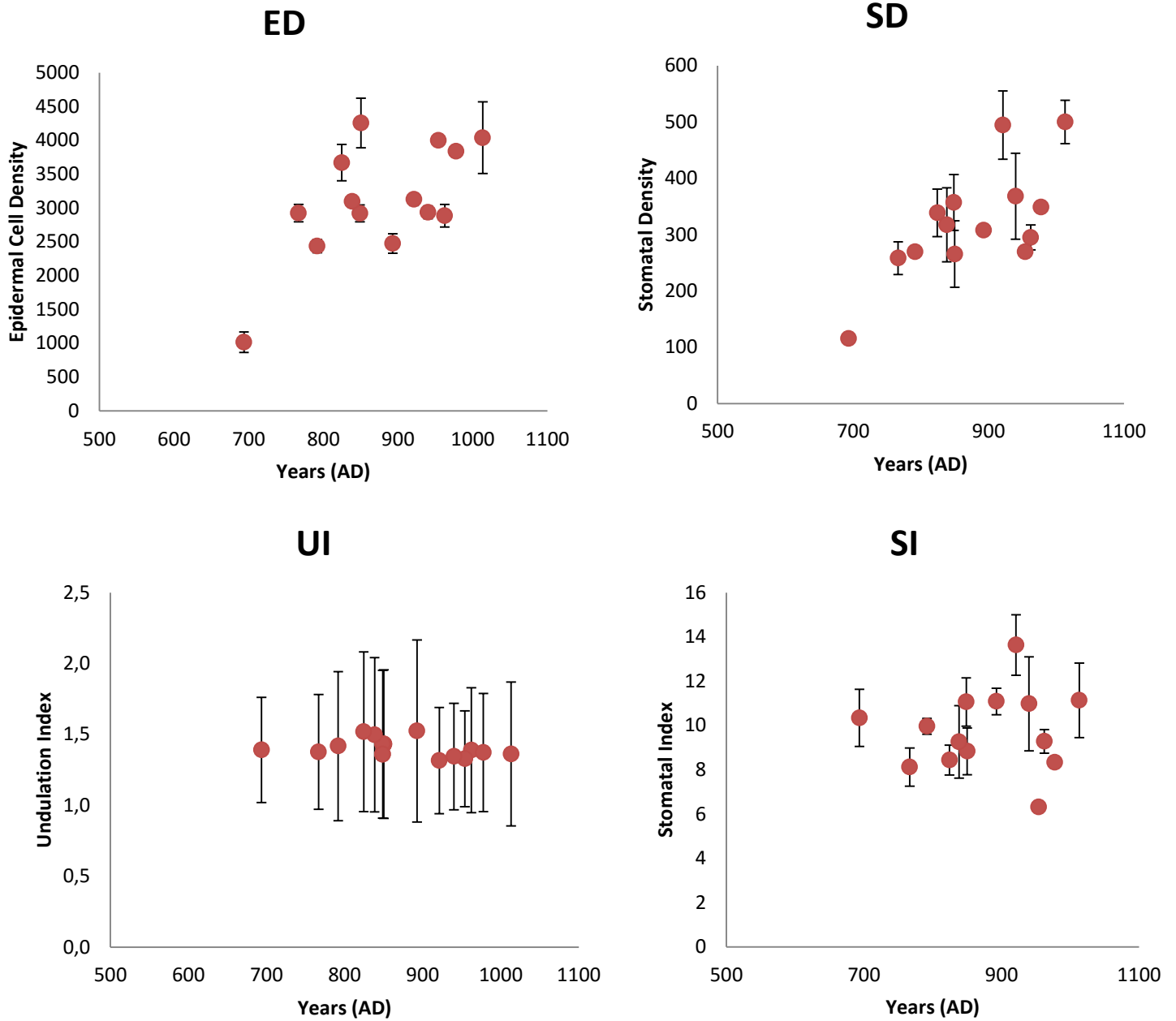
Fig. 5 : All results are plotted over time, using radiocarbon and OSL derived dates. (Upper left corner) Mean Epidermal Cell Density of Type 1. (Upper right corner) Mean Stomatal Cell Density of Type 1. (Lower left corner) Undulation Index of Type 1. (Lower right corner) Mean Stomatal Index of Type 1.

Analysis Type 1, Fabaceae

ED varies from mean minimum of roughly 1015 ED/mm2 and the maximum at about 4250 ED/mm2 (table 2)). The ED/mm2 is to be relatively low at 694 AD, after which it increases significantly and continues to stay high afterwards; although there appears to be some fluctuation in this higher density period. The mean SI balances out at around 10, but fluctuates between 6 and 14. The UI record, like the SI, show fluctuations and a relatively high value at 892 AD, although it seems to plummet faster after that year in the UI record. Both SI and UI do not record significant variation between 694 AD and the rest of the data. The SD, however, resembles the ED record showing an overall increasing trend over time, with significant low value at 694 AD. SD also includes small peaks around 921 and 1013 AD.

The sample at 694 AD could be considered an outlier due to the relatively low SD and ED values. When comparing a sample containing a high ED with this sample, significant similarity is present: differences in subsidiary cell size on both sides of the stomata are relatively small, one of the subsidiary cells has a single elongated epidermal cell connected to it (see figure 4, left and right labeled with the letter A), whereas the other subsidiary cell is connected with two epidermal cells, varying in size (one elongated (letter B), the other relatively widened (letter C)). Stomata shape is oval, with a clear opening of the pore visible.
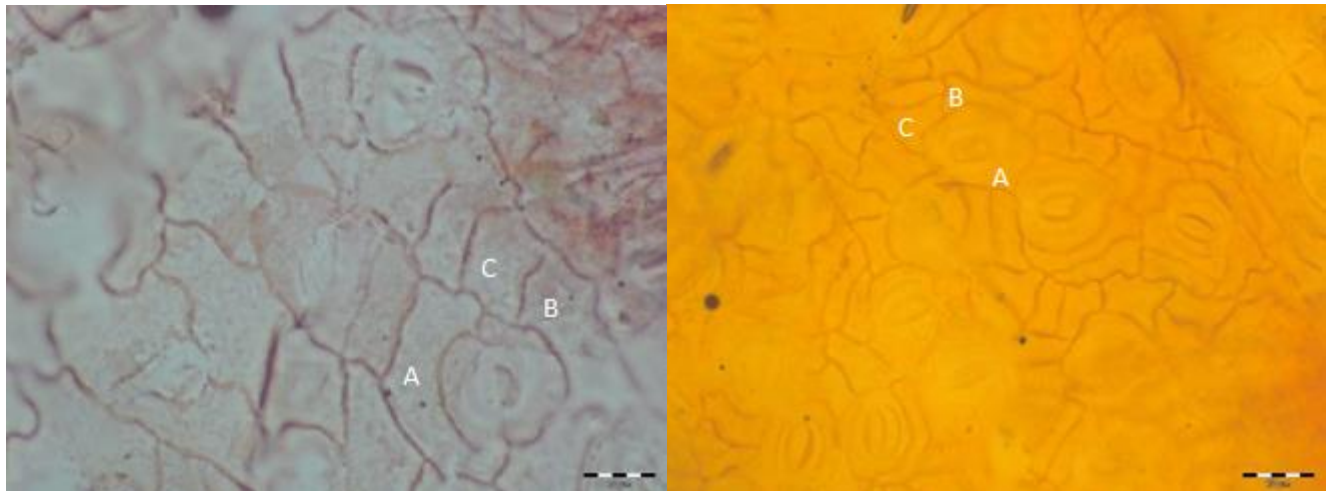

Fig. 4 : (Left) Sample 397 160 + 180 I, (*age 694* AD) Type 1, Fabaceae, (Right) Sample 380- 155 I, (*age 850 AD*) Type 1, Fabaceae. Scale bar represents 20 μm.

Type 2, Indeterminable

Samples allocated to type 2 all originate from one core. This core was taken in the transect on a previous fieldwork and is estimated to be deposited in 767 AD. As these samples were already investigated before more material was available, no determination based on colour or venation was done. When comparing the material with the recent material, no link could be found, although the size and shape of the stomata and epidermal cells do indicate the possibility of type

2 being a Fabaceae species. As all three samples are from one core and positioned at the same depth, no variation in time has been recorded. Instead, the three samples could be used to indicate possible fluctuation within locations.
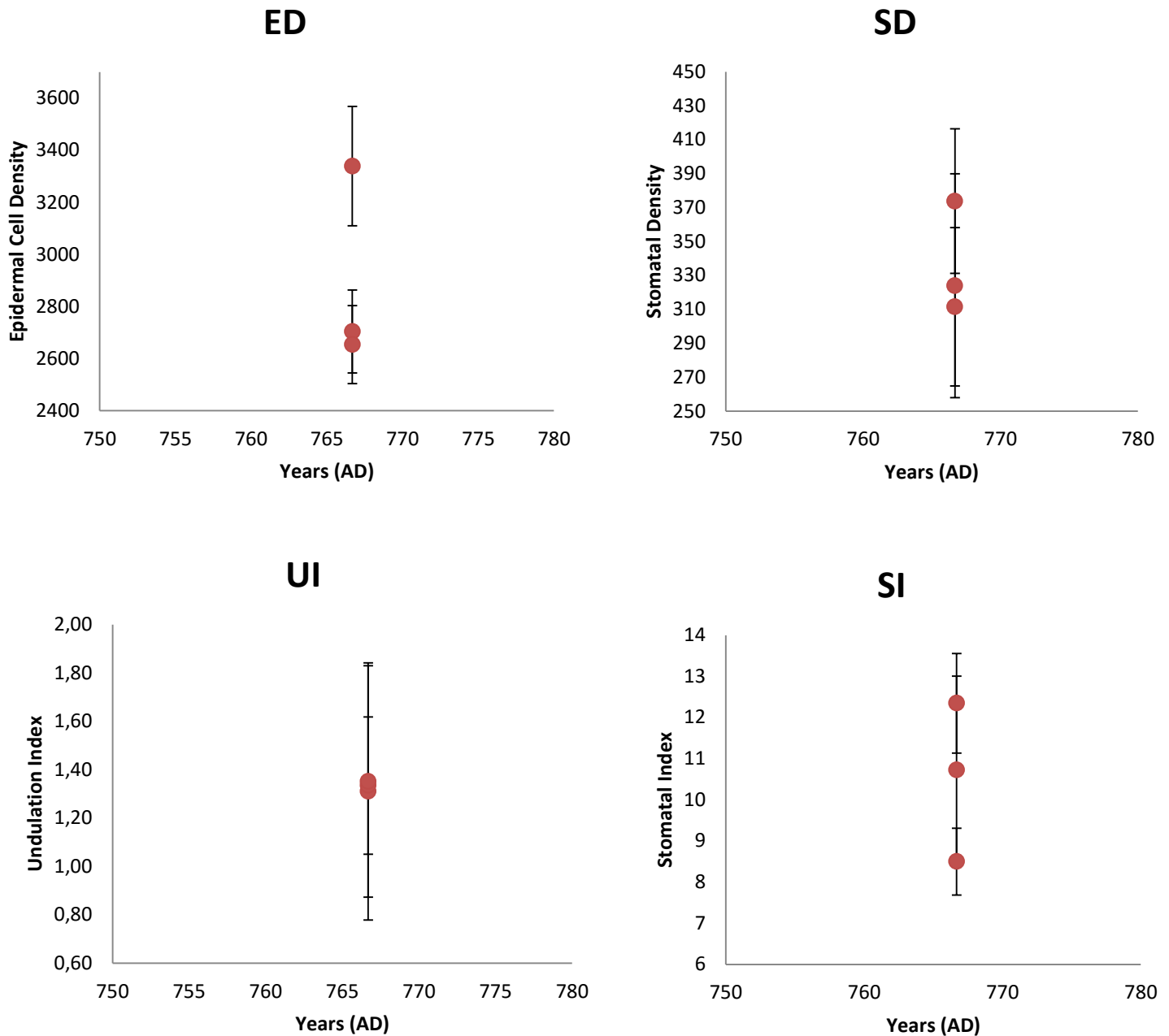

Fig. 5 : All results are plotted over time, using radiocarbon and OSL derived dates. (Upper left corner) Mean Epidermal Cell Density of Type 2. (Upper right corner) Mean Stomatal Cell Density of Type 2. (Lower left corner) Undulation Index of Type 2. (Lower right corner) Mean Stomatal Index of Type 2.

Analysis Type 2, Indet.

There appear to be very few differences between the samples belonging to Type 2. Only with the ED, one sample is not included within the error margins of the other two. When comparing the data with Type 1, Type 1 does seem to give the relatively same signal at 767 AD.

If Type 2 is also considered to be a Fabaceae species, these similarities between type 1 and 2 can be an indication that no species specific adaptations for drought stress are present in some species within this family.
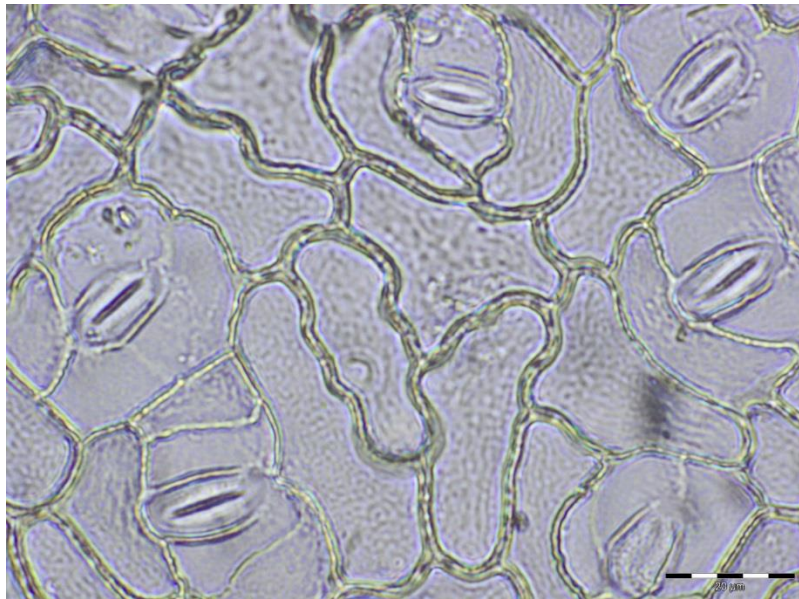
Fig. : Sample 193 171 SP 7 A, (age 767 AD) Type 2, indet. Possibly Fabaceae. Scale bar represents 20 μm.

Type 3, Indeterminable

A total of four samples are included in Type 3. Recent material investigated showed no clear similarities with Type 3. As it was not possible to determine Type 3 before bleaching by means of colour, clear differences are present compared to Type 1. Although the samples belong to type 3 were not present in the majority of the organic layers, the condition of the material was excellent and defined suitable for measuring xeromorphic characteristics in the abaxial.
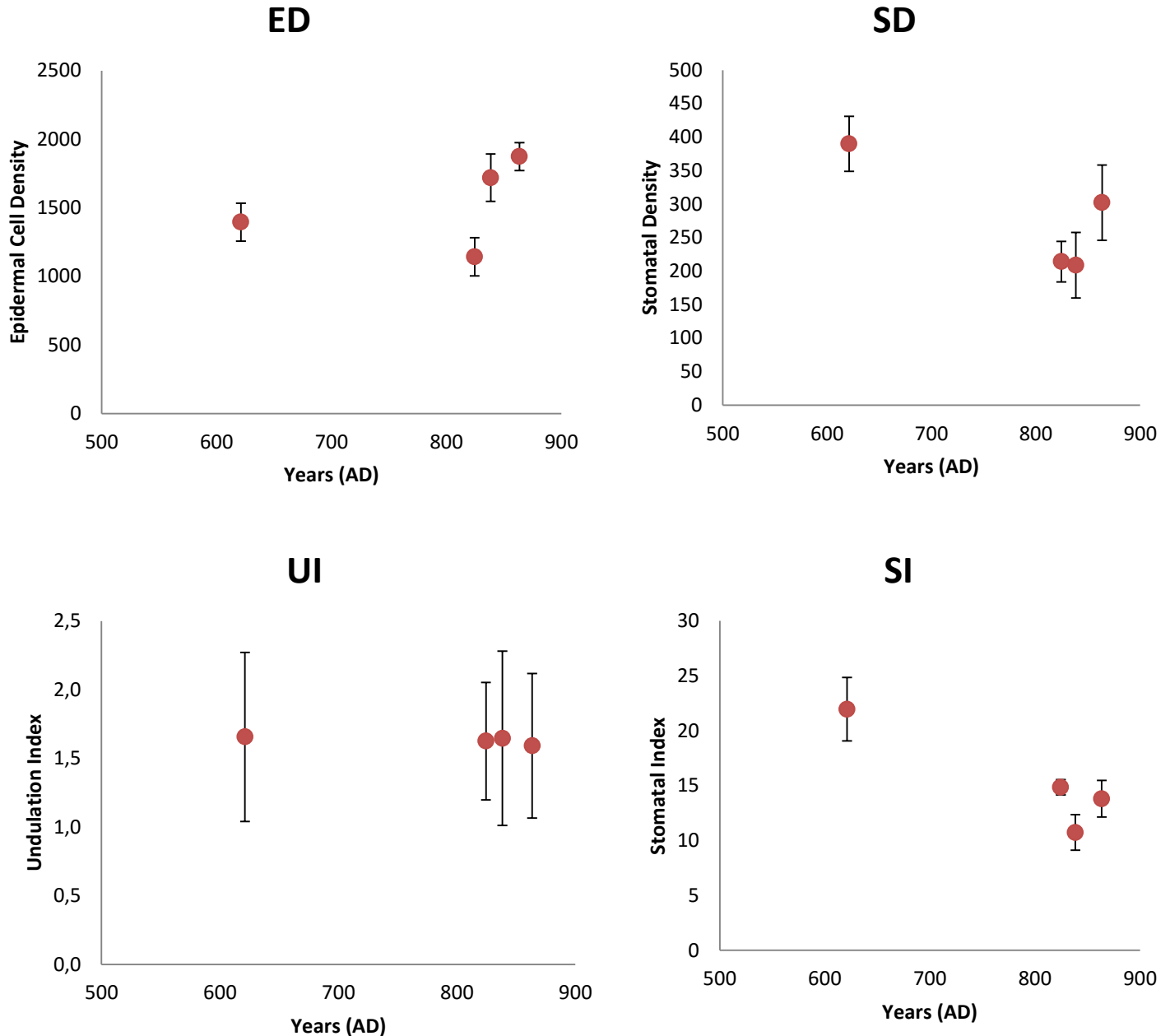
ED

SD

UI

SI

Fig. 5 : All results are plotted over time, using radiocarbon and OSL derived dates. (Upper left corner) Mean Epidermal Cell Density of Type 3. (Upper right corner) Mean Stomatal Cell Density of Type 3. (Lower left corner) Undulation Index of Type 3. (Lower right corner) Mean Stomatal Index of Type 3.

Analysis Type 3, Indet.

Results of the analysis are plotted in figure 6. ED varies from a minimum of roughly 1150 ED/mm2 and the maximum at about 1850 ED/mm2). The ED/mm2 gives relatively low result for 620 and 825 AD, with a steep increase after that. The mean SI and the SD/mm2 show the same trend; starting high at 620 AD and seems to fluctuate in the significantly lower values after that.

Characteristics of Type 3 includes a large variation existent in the shape of the subsidiary cell size on both sides of the stomata. Stomata shape is oval, and containing a pore opening which is sometimes partly closed by the Guard Cell.
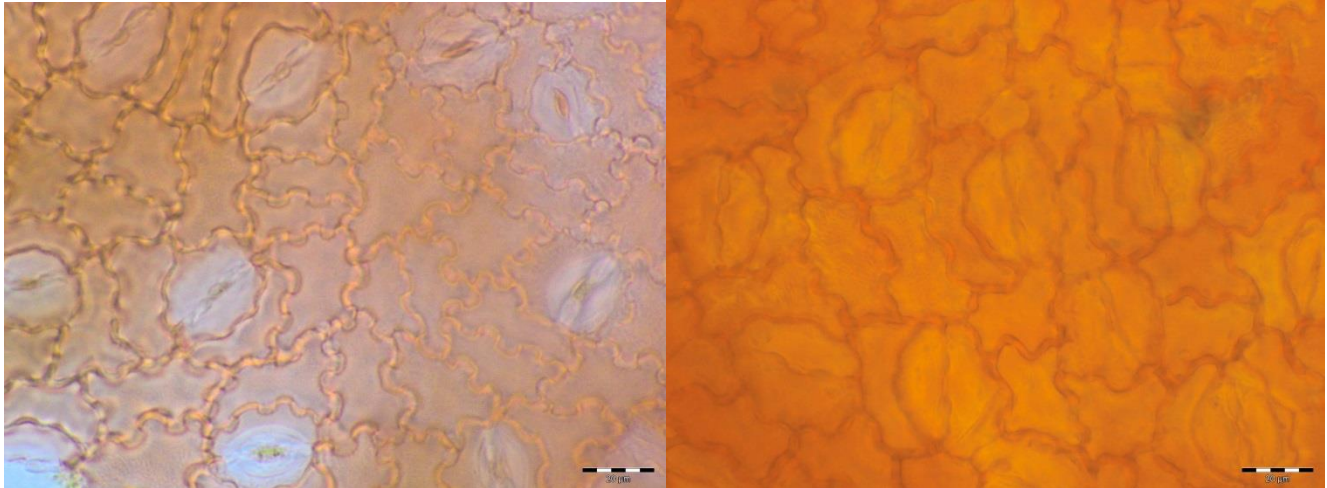

Fig. : (Left) Sample 426 255 I, (*age 621 AD*) Type 3. (Right) Sample 181 225 II, (*age 864 AD*) Type 3. Scale bar represents 20 μm.

Comparing Type 1 with Type 3

Both species do show a relatively low ED/mm2 before 750 AD which seems to increase at that point for Fabaceae and at ~ 830 AD for Type 3. No significant correlation can be detected between the UI, the SD and mean SI of the two species, possibly explainable by the low amount of data points in the Type 3 records. Due to the high error margins in the UI for both the types, the variation within this proxy are insignificant. SD, however, increases in the records of Type 1, whereas it clearly decreases in the Type 3 samples. SD record of the Type 1 Fabaceae shows a clear correlation with the ED, therefore the variation in stomata size is most likely linked with that of the epidermal cells. This could well result in the inapplicability of Type 1 stomata for CO_2 reconstruction. Type 3, however, shows relatively little variation in epidermal cell density, whereas a clear decrease in SD is recorded, which responds with the SI. Type 3, therefore, seems to be more applicable for CO_2 reconstruction than Type 1.

Type 4, Indeterminable.

A total of four leaf fragments are included in Type 4. Within the majority of these samples, certain species specific characteristics are no longer visible due to degradation or bleaching. Because of the absence of these characteristics, the samples cannot be determined or be allocated to one of the other types. Note that within Type 4 the samples are considered to belong to various species. The ED, SD, UI and SI are plotted in Appendix B.

Discussion

Probability of the results

Measuring

As there appeared to be a large variation in both the quantity and the quality of leaf material present in the different samples, certain samples seemed to be less suitable for reconstructing past precipitation changes. The quality of the leaf material investigated varied considerably. As some samples were too degraded to be measured, not every fragment was included in the results. Therefore, there is the possibility of missing certain signals in the record. Although the aim was to find seven independent areas for counting stomata cells and epidermal cells, the quality of certain samples made it sometimes impossible, decreasing this number in one case even to only one area. Also, one should realize that when including multiple fragments of the same species from one organic layer, there is the possibility of measuring two parts of the same leaf. Although the usable leaf material in the organic layers was not very abundant, Fabaceae did occur in the majority of the examined layers and proved to be usable in most cases. Due to relatively high error margins in the Undulation Index, the results of this index are not further interpreted in the discussion.

Dynamics groundwater level

Lowering of groundwater levels could result in certain organic layers to be located above the groundwater level and therefore become oxidized. This could result in the oxidation and rapid degradation of the leaf material situated in these layers. Ideally, samples are obtained as shallow as possibly, as the effects of degradation and variations in sedimentation are then reduced, however this was not always possibly. In Transect A, five cores have organic layers deposited just below the present groundwater level, inclining that the groundwater has not been lower than present levels in the past. Although it is unknown if the groundwater level has been higher at one point in time, this observation still suggests that the Maya Lowlands were located in a low energetic sea environment.

Dating

Multiple proxy dating has been used to achieve a time estimated of the beach ridges located at transect A. Both radiocarbon dating and optical stimulated luminescence (OSL) dating produce similar ages at this location. The formation of the beach ridge plain is chronological and expected to include a certain periodicity; assumptions can be made about the age of the ridges interlaying dated cores. The dated points were used to estimate the age of undated ridges by dividing the time between two dated locations with the amount of interlaying beach ridges.

Calibration Curve

Three different types of leafs have been analysed in this research, although more species were present in the organic material. Type 1 and 3 give a relatively similar result when comparing the ED, which could be a climatic response. The severity of this change will be investigated by creating a calibration curve. During the fieldwork, it was not yet possible to determine which species would be dominant in the organic layers, therefore a total of 32 different modern plant species have been sampled and determined. Most of the material was derived from the vegetation on the riverbanks of the Grijalva and the Usumacinta, although also vegetation on the beach and some samples from trees located at transect A were sampled. Assuming that the vegetation pattern of the area has not changed too drastically, it is possible to say that some of the organic material in the beach ridges was transported by one or both of the two river systems. Unfortunately, when investigating the recent material, no determination with the fossil material was possible. This could be explained due to changes in flora distribution over time, or alternations within the cuticle due to taphonomic processes.

Stomatal Index

Stomatal index has been used as a proxy for reconstructing atmospheric CO_2 concentration, whereas the undulation index tends to have a positive correlation with growing season properties (Wagner-Cremer et al., 2010). When including the SI results of the plant species investigated in this research, we expect some variation in the past CO_2 concentrations. Apparently, CO_2 values were relatively low, when a sudden change at around 800 AD resulted in the increase of the CO_2 concentration. Both *Salix* and Fabaceae show this result, verifying each other. Nevertheless, one should incorporate the changes in epidermal cell density as well before using the stomata index as a CO_2 proxy. As SI depends on the amount of epidermal cells changing in stomata cells, an increase of ED due to the lateral epidermal cell expansion will therefore result in the increase of the SD, limiting the applicability of SI as a CO_2 proxy.

Changes in the slope between the SD and the ED appear to be non-parallel for Type 3. A relatively small increase in ED over time, whereas SD tends to decrease. SI and SD show the same trend, possibly indicating that the effect of variations in ED on SI is limited. The drop in SD and SI, therefore, suggest a decrease in stomata formation over time. When using this SI, we find CO_2 concentrations to increase slowly during this time interval. The degree of this trend however remains uncertain. A calibration curve of modern leaf material is necessary to obtain more qualitative results

CO_2 reconstruction based on an arctic species of *Salix* has been done by Rundgren and Beerling (Rundgren et al., 1999). The time period covered by the *Salix* in this research only corresponds with 8 data points in the research done by Rundgren and Beerling. We assume a small increase from roughly 620 AD to 860 AD, based on the Mexican data. The CO_2 reconstruction from *Salix* seems to start dropping at 668 AD till 756 AD and then starts rising again till 840 AD, at which point the concentration of CO_2 appears to be higher than at 668 AD. Our data of Type 3, however, does not cover the area well enough to pinpoint the gap between 668 and 840 AD, although it did show the overall increase of CO_2 concentration in the atmosphere (figure 7).

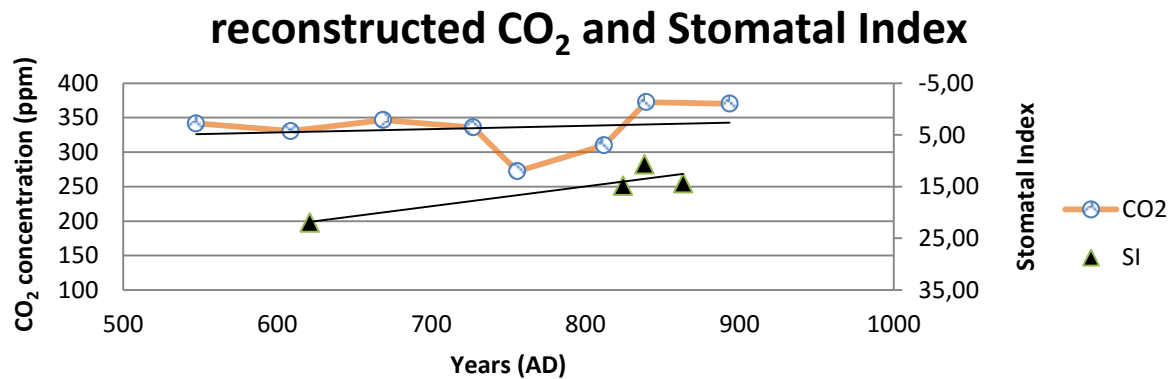# reconstructed CO$_2$ and Stomatal Index

Fig. 7: Comparison of CO$_2$ reconstruction by Rundgren and Beerling (1999) based on *Salix herbacea*, with the mean stomatal index of Type 3 species from the Maya Lowlands. Age model is based on radiocarbon dating at both sites and OSL dating at the Maya Lowlands. Note that there is a negative correlation between CO$_2$ concentrations and SI, therefore the SI axis is reversed.

Cuticle analysis as a precipitation proxy

Although this method has been used before the sub-tropical environment of Florida, it has yet to be tested on tropical environments. When assuming the method to be suitable for the tropical environment of the Maya Lowlands, other features might interfere to decrease its reliability. Sun leaves, on average, seem to contain a higher epidermal cell density than shade leaves; this due to the restriction of the lateral expansion of epidermal cells. (Wu et al., 2009 and Kürschner, 1997). Other morphological differences between sun and shade leaves include differences in the mesophyll anatomy and the undulation of the epidermal cells. Not making a distinction between the two leaf types, therefore, can result in inaccurate results. Although possibly interesting for future research, such a distinction has not been made in this research. During the fossilization process of oak leaf assemblages, there appears to be a preference for sun leaves over shade leafs, this preference is possibly explained by taphonomic processes (Kürschner, 1997). Although not investigated, we consider all organic leaf material to be derived from sun leaves, although the possible presence of shade leaves in the record cannot be excluded. Another reason for this assumption is that most of the species we have identified in the field from the family Fabaceae was either shrub or herb like, therefore not being affected by a difference in shade or sun leaves due to the open canopy of the shrubs. Type 1, however, shows resemblences with *Inga vera*, a tree belonging to the family Fabaceae. Subsequently, the presence of shadow leafs within type 1 could have an impact on its records.

Xeromorphic characteristics, such as the lateral expansion of epidermal cells, are formed during the growth period of the plant (Tichá, 1982; Wagner et al., 2007; Wagner et al., 2010). Therefore, a cuticle analysis based reconstruction of precipitation changes in the past only implies changes between growing seasons. Plant growth is influenced by changes in precipitation and temperature, parameters that are difficult to detect in tropic environments with low seasonality (Jones et al., 2009). The Maya Lowlands appear to contain the wettest weather conditions of Mexico, with an annual precipitation of

approximately 2010 mm at Villahermosa, Tabasco (World-Climate.com). Only the months February, March and April receive less than 100 mm of precipitation a month. June to November clearly is the wettest period in this region as the average precipitation in those months is 240,65 mm, individually ranging between 173 and 323,6 mm a month. At roughly 50% of those days, precipitation occurs. Although using cuticle analysis as a proxy for water availability has been successfully tested in the subtropics of Florida (Donders et al., 2004), there, a clear growing season was present during the winter. The assumption is that at the Maya Lowlands, leaf formation is present over the year, therefore not containing a typical growing season. Fluctuations in precipitation do occur, therefore, the results of the organic material could indicate differences in water availability within certain seasons, instead of a growing season with changing characteristics. We do expect to see the effects of El Niño winters and the formation of Northerns, which result in a decrease of the precipitation rate in southern Mexico. In order to prove this signal is apparent in our data, more research should be done involving recent plant material combined with known El Niño events. Previous research in lake sediments at the Yucatan Peninsula and speleothem records in Central America (Belize) estimated that a period of severe drought dominated the Maya Lowlands at the time of the demise of the Mayan civilization (around 800 AD). Although exact timing of the start of this dryer period is debatable, both proxies do indicate a rapid decrease in precipitation around this time period. In this research, precipitation changes have been reconstructed by means of cuticle analysis.

Epidermal cell Density

During periods with lower precipitation, lateral epidermal cell expansion is restricted, resulting in the formation of smaller epidermal cells (Bosabalidis and Kofidis, 2002; Li and Wang, 2003; Wagner et al., 2010). As the dimensions of the window used for measuring remain the same, a decrease in the epidermal cell size will result in the increase of the epidermal cell density. Evidently, the results of the epidermal cell density in both the Fabaceae and *Salix* start to increase from around 800 AD. This increase could be explained by a decrease in net precipitation in the area. Noticeable is that the results from the *Salix* species seem to lag with the Fabaceae, although this lag is inconclusive due to the limited amount of *Salix* samples incorporated. Fabaceae also reacts more drastically than *Salix*, an increase of +- 100% to an increase of +- 50%. This difference can be explained by the applicability of the species as a precipitation proxy, although without the presence of a calibration curve, this can only be speculated.

Speleothem records at the Yok Ballum Cave in Belize have identified multiple dryer periods between 800 AD and 1200 AD (Kennett et al., 2012), instead of one ongoing drought episode. There is some fluctuation within the record of Fabaceae, which seems to correlate nicely with the speleothem record (figure 8). The presence of a calibration curve could improve our understanding of the signal. A direct correlation between the two records has yet to be done, as more radiocarbon dating of the Maya Lowlands record might enhance the accuracy of the age model.
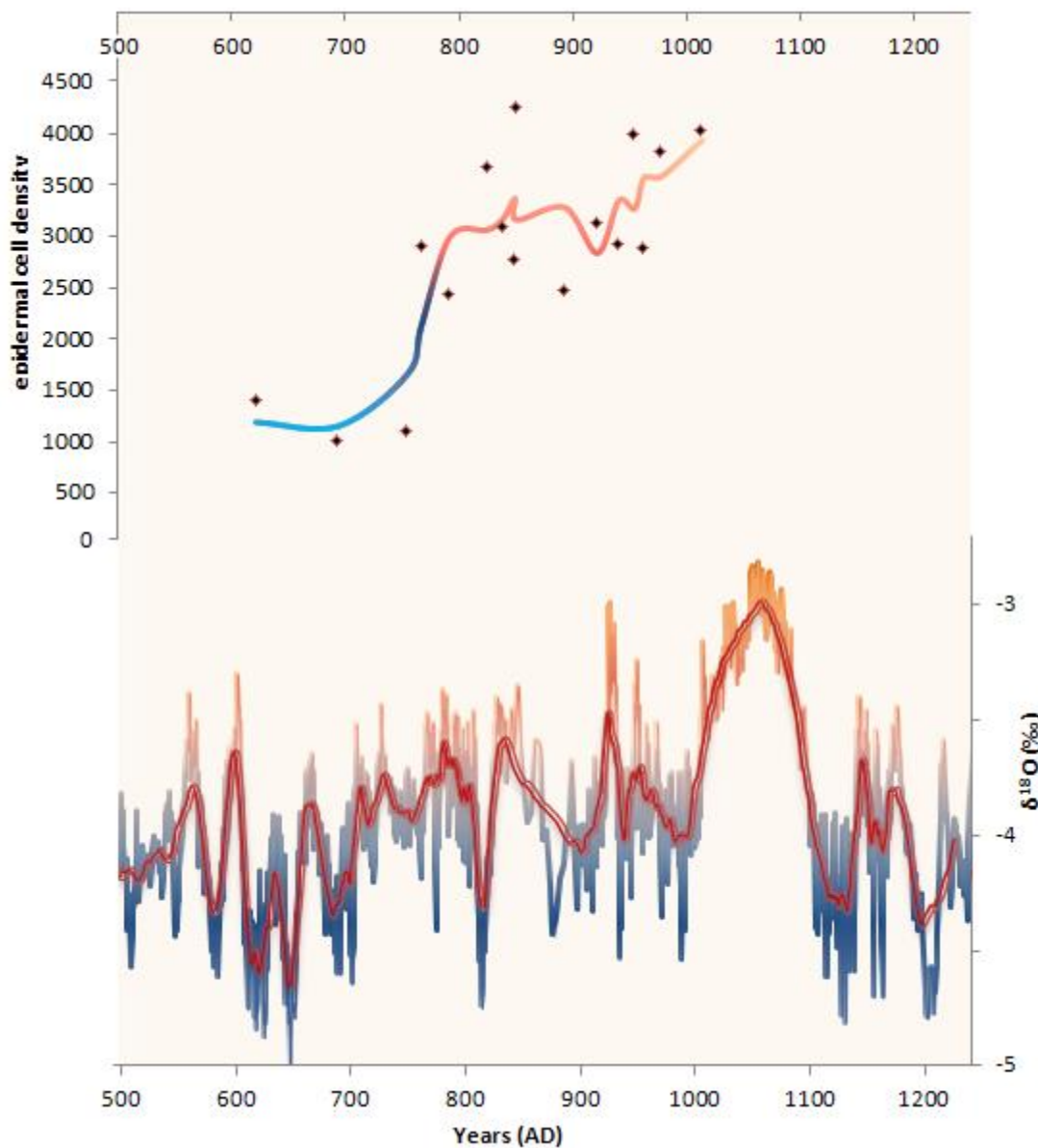
Fig. 8 : (Top) Epidermal Cell Density record at the Maya Lowlands (Tabasco, Mexico). 3 pt run. Avg., results show fluctuation in precipitation after the start of the drought episode. (Bottom) Speleothem $\delta^{18}O$ records from Yok Ballum Cave (Belize), 31 pt run. Avg., indicating multiple drought episodes during the TCP.

The speleothem record indicates a clear drop in $\delta^{18}O$ starting at around 1000 AD. Although the Fabaceae record stops around that period, it clearly indicates the continuing of a dry episode (figure 9A). The sediment record of Lake Chichancanab in Yucatan, Mexico (figure 9B and 9C), use $\delta^{18}O$ concentrations and sulphur contents in the sediment to indicate a dryer episode with an age range of ~AD 800 – 1000, with a drought maximum at 922 AD (Hodell et al., 1995). Our results seem to match with the start of this episode, although we do not see moist conditions at 1000 AD. Instead a continuing of the drought appears in the record, corresponding with the speleothem record. Hodell hypothesizes wet conditions after 1000 AD, although only the sulphur content seems to agree with this assumption. The $\delta^{18}O$ records seem to be higher after 1000 AD than before the drought episode, whereas the sulphur content seems to be significantly lower. As lake evaporation during dry periods is considerable at Lake Chichancanab, continuous drought might have an impact on the overall conditions of the lake, resulting in the inapplicability of sulphur content as a humidity proxy after 900 AD.
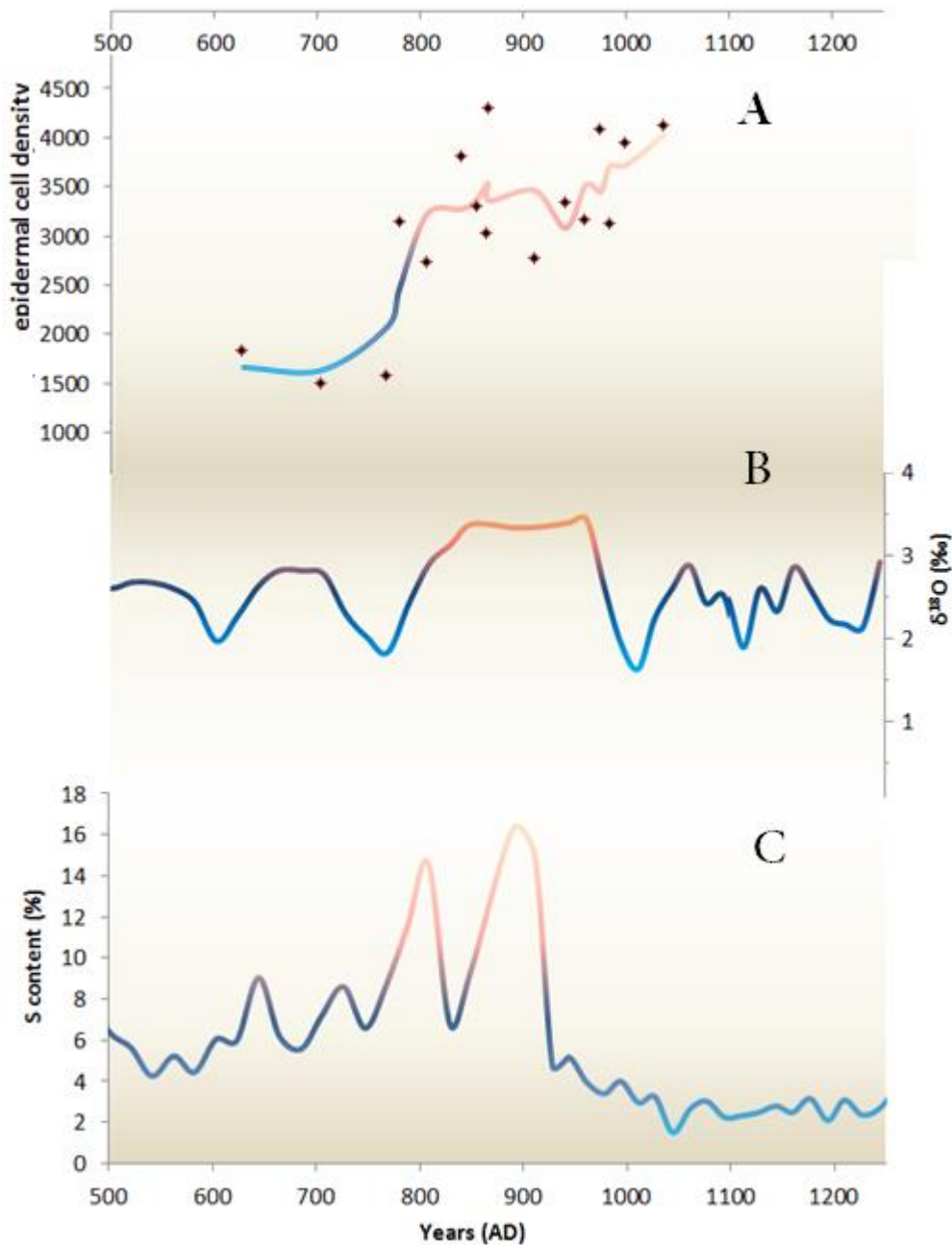
Fig. 9 : (A) Epidermal Cell Density record at the Maya Lowlands (Tabasco, Mexico), 3 pt run. Avg., showing a rapid increase at ~750 AD, indicating the start of a dryer period. Small interval occurs at around 920 AD, possibly showing variations in local precipitation and humidity levels at that time. (B) $\delta^{18}O$ concentration from Lake Chichancanab (Yucatan, Mexico), 3 pt run. avg., indicating a drought episode between 800 and 900 AD. (C) Sulphur content in percentages from Lake Chichancanab, indicating drought between 750 and 925 AD, with a sudden decreasing episode at 830 AD.

Conclusion

By using cuticle analysis of leaf fragments of the family Fabaceae and the genus *Salix*, we have been able to reconstruct precipitation changes during the TCP. The results point out to multiple drought episodes, providing new evidence for the assumed climatic changes in this time period. This research has successfully proved the applicability of cuticle analysis in tropical environments, therefore, indicating an entirely new proxy for the reconstruction of changes in precipitation and atmospheric CO_2 levels in such environments.

Acknowledgements

References

de Boer H.J., Lammertsma E.I., Wagner-Cremer F., Dilcher D.L., Wassen M.J.., Dekker S.C. (2011) Climate forcing due to optimization of maximal leaf conductance in subtropical vegetation under rising CO_2. *PNAS,* volume 108, issue 10, 4041-4046

Bosabalidis A.M., Kofidis G. 2002. Comparative effects of drought stress on leaf anatomy of two olive cultivars. *Plant Science*, volume 163, issue 2, 375-379

Cowan, C. P. (1983) Flora de Tabasco. Listados Floríst. *México*, volume 1, 1-123

Curtis J.H., Hodell D.A., Brenner, M. (1996). Climate variability on the Yucatan Peninsula (Mexico) during the past 3500 years, and implications for Maya cultural evolution. *Quaternary Research*, volume 46, 37–47.

Donders T.H., Wagner F., van der Borg K., de Jong A.F.M., Visscher H. (2004) A novel approach for developing high-resolution sub-fossil peat chronologies with ^{14}C dating. *Radiocarbon*, volume 46, issue 1, 445-463

Folan W.J., Hyde B.H. (1985) Climatic forecasting and recording among the ancient and historic Maya: an ethnohistoric approach to epistemological and paleoclimatological patterning. *Contributions to the Archaeology and Ethnohistory of Greater Mesoamerica, Southern Illinois University Press, Carbondale*, 15-48

Gunn J., Adams R.E.W. (1981) Climatic change, culture, and civilization in North America. *World Archaeology,* volume 13, issue 1, 87-100

Haug G.H., Günther D., Peterson L.C., Sigman D.M., Hughen K.A., Aeschlimann B. (2003) Climate and the Collapse of Maya Civilization. *Science*, volume 299, 1731-1735

Hodell D.A., Brenner M., Curtis J.H. (2005) Terminal Classic drought in the northern Maya lowlands inferred from multiple sediment cores in Lake Chichancanab (Mexico). *Quaternary Science Reviews,* volume 24, 1413-1427

Hodell D.A., Curtis J.H., Brenner M. (1995) Possible role of climate in the collapse of Classic Maya civilization. *Nature*, volume 375, 391-394

Idu M., Olorungemi D.I., Omonhinmin A.C. (1999) Systematics value of stomata species of *Fabaceae* in some Nigerian hardwood. *Plant Biosystem*, volume 134 issue 1, 53-60

Jones P.D., Briffa K.R., Osborn T.J., Lough J.M., van Ommen T.D., Vinther B.M., Luterbacher J., Wahl E.R., et al.(2009). High-resolution palaeoclimatology of the last millennium: A review of current status and future prospects. *The Holocene*, volume 19, 3–49

Kennett D.J., Breitenbach S.F.M., Aquino V.V., Asmerom Y., Awe J., Baldini J.U.L., Bartlein P., Culleton B.J., Ebert C., Jazwa C., Macri M.J., Marwan N., Polyak V., Prufer K.M., Ridley H.E., Sodemann H., Winterhalder B., Haug G.H. (2012) Development and disintegration of Maya political systems in response to climate change. *Science*, volume 338, 788-791

Kürschner W.M. (1997) The anatomical diversity of recent and fossil leaves of the durmast oak (*Quercus petraea* Lieblein/*Quercus pseudocastanea* Goeppert): implications for their use as biosensors of paleoatmospheric CO_2 levels. *Review of Palaeobotany and Palynology*, volume 96, 1-30

Lachniet M.S., Bernal J.P., Asmerom Y., Polyak V., Piperno D. (2012) A 2400-yr rainfall history links climate and cultural change in Mexico. *Geology,* volume 40, issue 3, 259-262

Lammertsma E.I., de Boer H.J., Dekker S.C., Dilcher D.L., Lotter A.D., Wagner-Cremer F. (2011) Global CO_2 rise leads to reduced maximum stomatal conductance in Florida vegetation. *PNAS,* volume 108, issue 10, 4035-4040

Li C., Wang K.(2003) Differences in drought responses of three contrasting *Eucalyptus microtheca* F. Muell. Populations. *Forest Ecology and Management*, volume 179, issues 1-3, 377-385.

Lowe J.W.G. (1985) The dynamics of Apocalypse: A systems simulation of the classic Maya collapse. *University of New Mexico Press, Albuquerque*

Méndez M., Magaña V. (2010) Regional aspects of prolonged meteorological droughts over Mexico and Central America. *Journal of Climates*, volume 23, issue 5, 1175-1188

Metcalfe S.E., Jones M.D., Davies S.J., Noren A., Mackenzie A. (2010) Climate variability over the last two millennia in the North American Monsoon region, recorded in laminated lake sediments from Laguna de Juanacatlan, Mexico. *The Holocene,* volume 20, issue 8, 1195-1206Psuty N.P. (1965) Beach ridge

development in Tabasco, Mexico. *Annals Association of American Geographers*, volume 55, issue 1, pp. 112–124

Magaña V.O., Vázquez J.L., Pérez J.L., Pérez J.B. (2002) Impact of El Niño on precipitation in Mexico. *Geofísica Internacional*, volume 42, issue 3, 313-330

Molinari J., Knight D., Dickinson M., Vollero D., Skubis S. (1997) Potential vorticity, easterly waves and eastern Pacific tropical cyclogenesis. *Monthly Weather Review*, volume 125, issue 10, 2699-2708

Rundgren M., Beerling D.J. (1999) A Holocene CO_2 record from the stomatal index of subfossil *Salix herbacea* L. leaves from northern Sweden. *The Holocene,* volume 9, 509-513

Salisbury E. J. (1927). On the causes and ecological significance of stomatal frequency, with special reference to the woodland flora. *Philosophical Transactions of the Royal Society of London, B, Biological Sciences,* volume 216, 1-65

Stahle D.W., Villanueva Diaz J., Burnette D.J., Cerano Paredes J., Heim Jr. R.R., Fye F.K., Acune Soto R., Therrell M.D., Cleaveland M.K., Stahle D.K. (2011) *Geophysical Research Letters,* volume 38, L05703

Transviña A., Barthon E.D. (1997) Los "Nortes" del Golfo de Tehuantepec: la circulación costera inducida por el viento. *Contribuciones a la Oceanografía Física en México*. Monografía 3, Unión Geofísica Mexicana, 25-46

Tamura T. (2012) Beach ridges and prograded beach deposits as palaeoenvironment records. *Earth-Science Reviews,* volume 114, issues 3-4, pp 279-297

Tichá I. (1982) Photosynthetic characteristics during ontogenesis of leaves: 7. Stomata density and sizes. *Photosynthetica*, volume 16, 375-471

Wagner-Cremer F., Donders T.H., Visscher H. (2010) Drought stress signals in modern and subfossil *Quercus laurifolia* (Fagaceae) leaves reflect winter precipitation in southern Florida tied to El Niño–Southern Oscillation activity. *American Journal of Botany*, volume 97, 753-759

Wagner-Cremer F., Finsinger W., Moberg A. (2010) Tracing growing degree-day changes in the cuticle morphology of *Betula nana* leaves: a new micro-phenological palaeo-proxy. *Journal of Quaternary Science,* Volume 25, issue 6, 1008-1017

Wagner F., Visscher H., Kürschner W.M., Dilcher D.L. (2007) Influence of ontogeny and atmospheric CO_2 on stomata parameters of *Osmunda regalis*. *Courier Forschungsinstitut Senckenberg*, volume 258: 183–189

Wu J., Bainian S., Yu-Sheng L., Snaping X., Zhicheng L. (2009) A new species of *Exbucklandia* (Hamamelidaceae) from the Pliocene of China and its paleoclimatic significance. *Review of Palaeobotany and Palynology*, volume 155, issues 1-2, pp 32-41